Nano Energy (2015) 12, 258–267

Available online at www.sciencedirect.com

ScienceDirect

journal homepage: www.elsevier.com/locate/nanoenergy

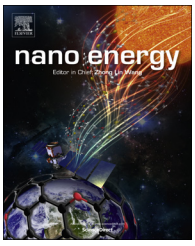

SHORT COMMUNICATION

Electrochromo-supercapacitor based on direct growth of NiO nanoparticles

Guofa Cai, Xu Wang, Mengqi Cui, Peter Darmawan, Jiangxin Wang, Alice Lee-Sie Eh, Pooi See Lee*

School of Materials Science and Engineering, Nanyang Technological University, 639798, Singapore

Received 8 November 2014; received in revised form 9 December 2014; accepted 22 December 2014
Available online 31 December 2014

KEYWORDS
Nickel oxide;
Energy storage;
Electrochromism;
Nanoparticle;
Electrochromo-supercapacitor

Abstract
In this paper, uniform NiO nanoparticles on different substrates were successfully synthesized by a simple and low-cost solvothermal method. The high capacitance (1386 F g^{-1} at 1 A g^{-1}) and excellent rate capability were achieved for NiO nanoparticle film as supercapacitor electrode. A large optical modulation (63.6% at 550 nm), high coloration efficiency (42.8 cm^2 C^{-1} at 550 nm) and good cycling stability can be achieved when the same NiO nanoparticles are used for electrochromic application. The excellent electrochemical performance is attributed to the uniform nanoparticles morphology and stable chemical bonding of the NiO nanoparticle on the substrates, which shorten the ion diffusion length and greatly facilitated the charge transfer both at the contact interfaces and within the electrode materials during the electrochemical process. In addition, we present a smart supercapacitor which function as a regular energy storage device and simultaneously monitor the level stored energy by visual changes. The findings present great promise for NiO nanoparticle film as practical electrode materials as chromo-supercapacitor.

Introduction

The escalating problems of energy and environment require society to move towards sustainable and renewable resources. Harvesting, converting, storing and saving renewable energy are the most important energy solution strategies [1–5]. Supercapacitors also known as electrochemical capacitors are gaining increasing attention due to their high power density, rapid charging/discharging rate, superior rate capability, long cycle life and the ability to balance the need of high energy density of battery and fast power delivery of capacitor. However, while major progress has been achieved in the theoretical and practical aspect of supercapacitors recent years, supercapacitors still suffer from high production cost, compromised rate capacitance and reversibility [6–10].

On the energy conservation spectrum, smart glass based on electrochromics potentially reduce 16% of peak electricity load through modulation of transmitted light and solar

*Corresponding author. Tel.: +65 67906661.
E-mail address: pslee@ntu.edu.sg (P.S. Lee).

http://dx.doi.org/10.1016/j.nanoen.2014.12.031
2211-2855/

heat, providing indoor comfort and energy efficiency simultaneously [11–13]. The optical modulation of electrochromics such as transmittance, reflectance and absorptance is achieved by an electric field assisted insertion and extraction of cations and electrons. Unfortunately, short life time, low chromatic contrast, long switching time and low coloration efficiency limit its widespread deployment. To overcome the drawbacks of the supercapacitor and smart glass, tremendous research effort on the development of nanostructure materials for electrochemical active electrodes has been pursued.

Recently, nickel oxide (NiO) as a typical electrode material has been intensively researched because of its superior electrochemical performances in both supercapacitors [14,15] and electrochromic devices [16]. Synthesis of high surface area NiO nanoparticles film obtained from sol-gel [17], electrodeposition [18] and spray pyrolysis [19] has facilitated a reduced ion diffusion length and improved electrolyte penetration within the NiO nanoparticle layer. However, most of the pure NiO films suffer from poor cycling stability due to the poor adhesion with the transparent conducting substrate such as indium tin oxide (ITO). For example, Zayim et al. [17] fabricated NiO films by the spin-coating technique, the films gradually degraded after 500 cycles. Xia et al. [20] prepared highly porous NiO thin films on ITO glass by a simple chemical bath deposition method in combination with a heat-treatment process. Although the films exhibit large optical modulation up to 82% and the high coloration efficiency (*CE*) of 42 $cm^2\,C^{-1}$, parts of the film detached from the substrate after 300 cycles and the film electrode started to break down. Recently, Cai et al. [21] synthesized nanostructured NiO thin films by simple and efficient electrodeposition in a choline chloride-based ionic liquid. The films exhibit fast switching speed and high *CE*, but the film started to fall off the ITO substrate after 600 cycles. In addition, the synthesis of the uniform NiO nanoparticles is not easy due to the existing approaches plagued by complex procedures, unwanted side-reaction, small yield, large particle size distribution, and required a subsequent thermal treatment. For instance, Jahromi et al. [22] synthesized NiO nanoparticles by a sol-gel method in a gelatinous medium. The reaction process required a subsequent thermal treatment, and the NiO nanoparticles exhibited a broad particle size distribution. Li et al. [23] found that the reaction between hexadecylamine and nickel acetylacetonate was rapid and hard to control, resulting in the formation of a black Ni precipitate exclusively. Recently, Liang et al. [24] synthesized the NiO based on ligand protection method, but the yield of the product was small. Furthermore, the experiment process is complex due to the NiO powder need to be precipitated out and further purify by adding some solvents. In addition, the NiO films were prepared by a two-step fabrication procedure. We have previously introduced the use of linear polyethylenimine treatment to provide bonding that proves to enhance the cycling stability of V_2O_5 and WO_3 sol-gel films on ITO [25,26]. Therefore, it is of great importance to design and fabricate high-quality electrode materials with chemical compatibility to the surface of the ITO substrates.

Herein, we report direct growth of uniform NiO nanoparticles on different substrates using a simple and low-cost solvothermal method. The uniform NiO nanoparticle films were fabricated without further thermal treatment. We evaluate the electrochemical properties of the NiO nanoparticles in the applications of supercapacitor and electrochromics. The uniform NiO nanoparticle films exhibit excellent electrochemical performance, including excellent rate capability, high capacitance, large optical modulation, high coloration efficiency and super-long cycle life. We demonstrate an electrochromo-supercapacitor that changes color to reflect the state of charging based on the NiO nanoparticles electrode.

Experimental section

Tert-butanol (anhydrous, $\geq$99.5%), nickel acetylacetonate (95% purity), nickel nitrate hexahydrate and Triton™ X-100 were purchased from Sigma-Aldrich. Isopropyl alcohol (95% purity) was purchased from Aik Moh Paints & Chemicals Pte Ltd. (95% purity). Polyethylene glycol 200 and ammonia solution (29%) were obtained from Merck. All chemicals were used without further purification.

Preparation of uniform NiO nanoparticles film

Firstly, nickel foam and ITO-coated glass were washed with acetone, de-ionized water, and finally with ethanol in an ultrasonic bath for 10 min. For ITO-coated glass substrate, a NiO seed layer needs to be prepared before growth of uniform NiO nanoparticles. The NiO seed layer was prepared on ITO-coated glass through a spin coating method. The coating solution was prepared according to the literature [27]. Briefly, 1.7 g nickel nitrate hexahydrate was dissolved into 60 ml of equal amounts of isopropanol alcohol and polyethylene glycol 200. Then 2 ml ammonia solution (29%) and 1 ml Triton™ X-100 were added to the above solution under stirring to form nickel hydroxide colloid solution. The solution was further stirred for 30 min and the final solution was used to coat on the ITO substrates by a spin-coater. The spin coating processes were performed at 3000 rpm for 60 s and repeated for 2 times. The coated substrates were heated at 350 °C for 20 min during each coating process. For growth of uniform NiO nanoparticles on different substrates, the reaction solution was prepared through a modified approach on a previously reported method [28]. Briefly, 0.39 g nickel acetylacetonate was added into 42 ml tert-butanol under magnetic stirring forming a light green suspension. Afterwards, the suspension obtained was transferred into a Teflon lined stainless autoclave. The nickel foam and ITO-coated glass with the NiO seed layer were placed vertically in the autoclave, and then the autoclave was sealed and heated at 200 °C for 24 h. After synthesis, the autoclave was cooled to room temperature under natural cooling. The substrates were taken out, rinsed extensively with deionized water and allowed to dry in ambient air. The precipitates in the solution were also collected and treated the same way for Fourier transform infrared spectra (FTIR) characterization.

Sample characteristics

X-ray diffraction (XRD, Shimadzu discover diffractometer with CuKα-radiation (λ=1.5406 Å)), scanning electron microscopy (SEM, JEOL 7600F), and transmission electron microscopy

(TEM, JEOL 2010) are used to identify the morphology, structure and composition of the products, respectively. X-ray photoelectron spectroscopy (XPS) analysis of the NiO films on ITO substrates was performed using VG ESCALab 220i-XL Imaging XPS last calibrated in Mar 2014. Mg Kα X-ray ($h\nu$=1253.6 eV) from a twin anode X-ray gun was employed using a large area lens mode for analysis with photoelectron take-off angle of 90° with respect to surface plane. The analysis area is approximately 4×4 mm^2 while the maximum analysis depth lay in the range of 4–8 nm. FTIR spectroscopy was performed on a Frontier™ FT-IR/NIR Spectrometer (PerkinElmer, Inc.). The spectra were recorded between 4000 and 400 cm^{-1} at a resolution of 4 cm^{-1}.

Electrochemical characterization

The electrochemical measurements were carried out in a three-electrode electrochemical cell containing 1 M KOH aqueous solution as the electrolyte. Cyclic voltammetry (CV) and chronoamperometry (CA) measurements were performed on an Autolab PGSTAT 30 potentiostat. CV measurements were carried out at different scanning rates between 0 V and 0.6 V at 25 °C with the Ag/AgCl as the reference electrode and Pt foil as counter-electrode. The galvanostatic charge–discharge test was carried out from 0 to 0.5 V vs. Ag/AgCl. The transmission spectra of NiO thin films in the fully colored and fully bleached states were measured over the wavelength range from 300 to 900 nm with a SHIMADZU UV-3600 spectrophotometer. The electrochemical impedance spectroscopy (EIS) tests were conducted in the frequency range of 100 kHz to 0.01 Hz with the signal amplitude of 5 mV under open circuit voltage using Solartron 1470E.

Results and discussion

Microstructure characteristiscs

The phase information of products was characterized by XRD, as shown in Figure 1. After subtracting the diffraction peaks of substrates, both the films show diffraction peaks at 2θ degrees of 37.78°, 43.31° and 62.74°, which can be assigned to (111), (200) and (220) reflections of the cubic NiO phase (JCPDS 00-047-1049), respectively.

SEM images of the films are shown in Figure 2. It can be clearly seen that the uniform NiO granules can grow on both of nickel foam and NiO seed layer covered ITO glass substrates. The average grain size of the granules was estimated to be 30–40 nm. Some voids opened between these granules are also observed. These voids between grains can allow the electrolyte to penetrate through the film and shorten the ions diffusion lengths within the bulk of NiO. It is noteworthy that the NiO seed layer plays the key role for the uniform NiO granules grown on ITO-coated glass substrates. Before solvothermal reaction, a uniform NiO seed layer with a thickness of about 20 nm was prepared on ITO-coated glass through the sol–gel method (Figure S1a and b in Supporting information). It can be seen that the granules grown on the NiO seed layer covered substrate (Figure 2c and d) are significantly larger than the granules grown on bare ITO substrate (Figure S1c and d in Supporting information). In addition, the thickness of the

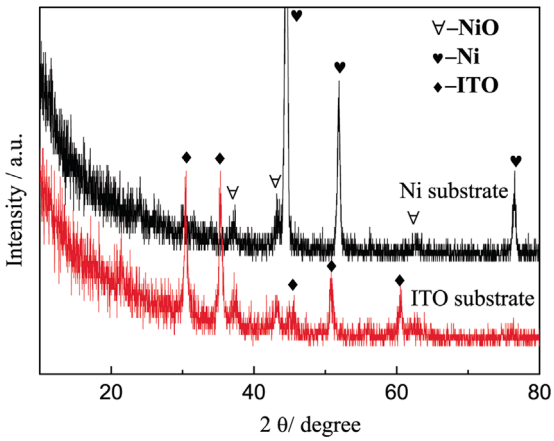

Figure 1 XRD patterns of the NiO films prepared on different substrates from the reaction of nickel acetylacetonate in tert-butanol at 200 °C for 24 h.

NiO film with seed layer is about 380 nm which is larger than that of the NiO film with bare ITO (about 180 nm), with the same growth duration. The uniform and rapid growth of NiO layer induced by the seed layer covered substrate is mainly due to the matching lattice structure and polar nature of the NiO seed surface. Figure 3a is a typical low-magnification TEM image of the NiO product scratched from the ITO substrate and re-dispersed in ethanol solution, showing uniform granules possessing an average diameter of 30–40 nm, in good consistency with SEM results. Furthermore, high-resolution TEM (HRTEM) image further verified that the granules were assembled from smaller nanoparticles with a diameter of 4–6 nm (Figure 3b). In addition, the HRTEM exhibits lattice-resolved fringes with spacing between adjacent lattice planes of 0.24 nm, corresponding to the (111) planes of cubic NiO.

XPS was performed to analyze the chemical compatibility between the NiO film and ITO with seed layer. Figure 4a shows XPS survey spectra of NiO seed layer and NiO film with seed layer, both on ITO substrates. The XPS survey spectra of NiO seed layer contains Ni, O, In, some traces of C and Sn. The elements of In and Sn come from the ITO substrate, which indicates the NiO seed layer is very thin and contains some porosity that exposes the ITO surface. However, after growth of NiO nanoparticles film on the seed layer by solvothermal reaction, the XPS survey spectra of NiO film only contains Ni, O and some traces of C. The disappearance of In and Sn in this spectrum indicates that the NiO nanoparticles film provides full coverage on the ITO surfaces. In addition, the binding energy peaks of In 3d and In 4d are located at 444 and 17.5 eV, respectively, which are lower than those of In 3d and In 4d in pure ITO glass reported in previous literatures [29–31]. The work-function measurement of the ITO/NiO structure has been found to be higher than that of the ITO alone according to the literature [32], which indicates that there exists chemical bonding at the contact interface between the seed layer and the ITO substrate. Figure 4b shows the highly resolved narrow scans Ni 2p core-level spectra of NiO seed layer and NiO film with seed layer. Ni $2p_{3/2}$ peak includes two components for both samples, one stronger peak at 854 eV due to Ni^{2+} in Ni–O

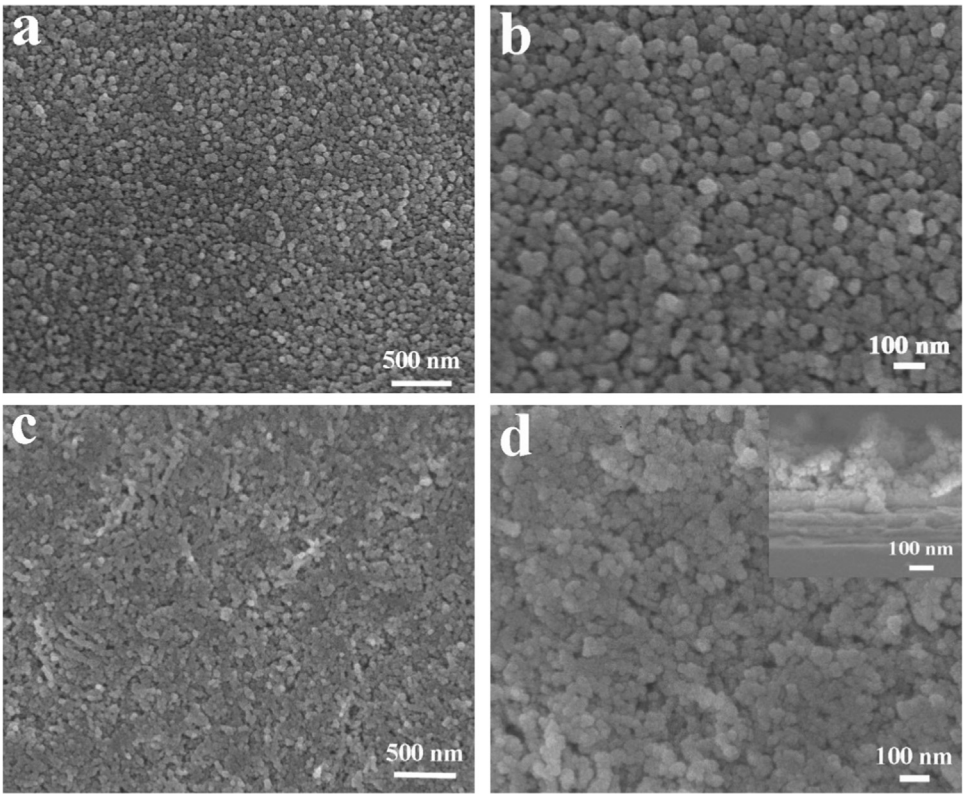

Figure 2 (a, b) SEM images of the NiO nanoparticles growing on nickel foam, and (c, d) ITO glass with the NiO seed layer.

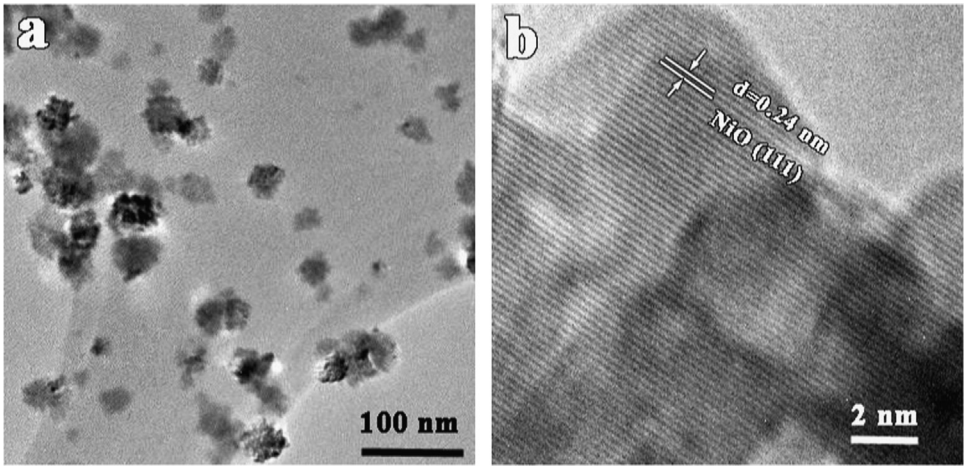

Figure 3 (a) Low magnification and (b) high magnification TEM images of the NiO nanoparticles scratched from the NiO film and re-dispersed in ethanol solution.

bonds and a weaker peak at 856 eV due to Ni–OH bonds, respectively [28,33,34]. The Ni–OH bonds mainly come from NiOOH or tert-butoxide groups attached to the surface of NiO [28]. It illustrates that the product present is mainly NiO, and possibly small amount of NiOOH is also present on the surface of NiO film layer. In C 1s spectra of both films, three most prominent components can be clearly seen in Figure 4c. The peak at 284.4 eV is assigned to C–C, and the other two peaks at 286 eV and 288 eV are assigned to species of C–O corresponding to hydroxyl and epoxy, and the component of C = O corresponding to carboxyl. In addition, the binding energy of C–C bond in NiO film with seed layer is larger than that of the NiO seed layer; this could arise from the residual reaction of tert-butanol with NiO.

FTIR analyses were used to further confirm the chemical identity of the NiO nanoparticles as shown in Figure 5. The broad band at around 3429 cm^{-1} is characteristic of the stretching vibration of hydrogen bonded hydroxyl groups (O–H) located in the interlamellar space of the sample. The bands at 2921 and 2849 cm^{-1} are respectively assigned to the asymmetric and symmetric stretching vibrations of methylene (CH_2) in the alkyl chain. The strong bands at 1398 and 1569 cm^{-1} correspond to the asymmetric and symmetric stretching vibrations of the carboxylic group

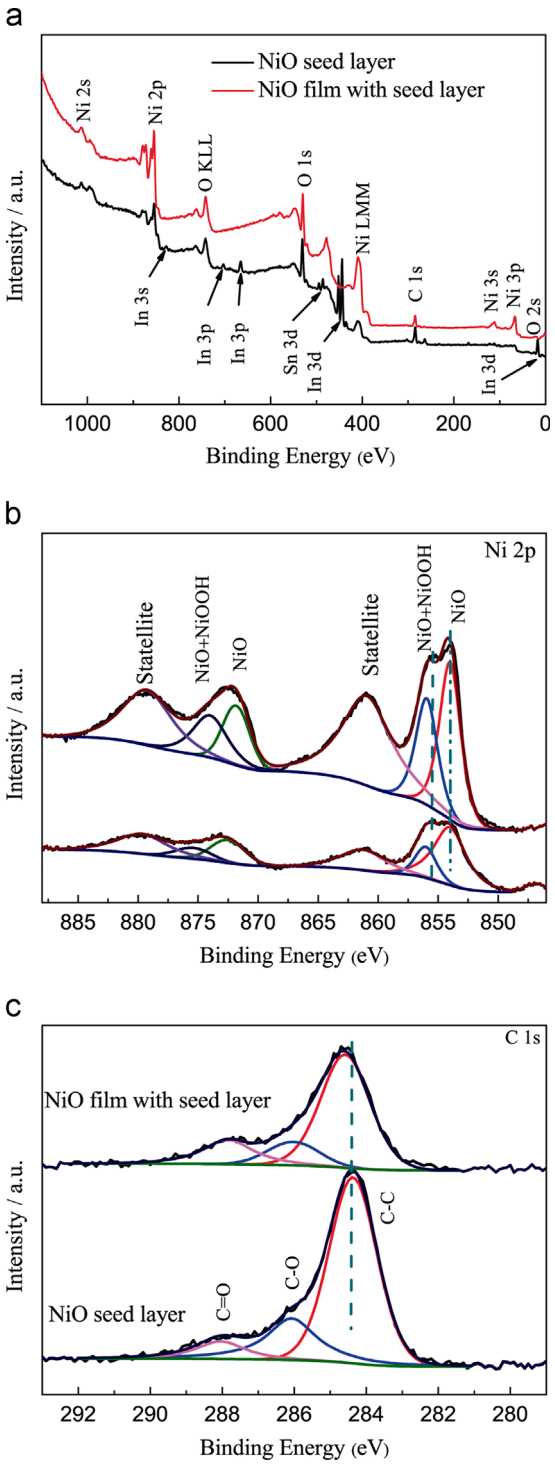

Figure 4 XPS spectra of NiO seed layer and NiO film with seed layer. (a) Survey spectra, (b) narrow scans Ni 2p core-level spectra, and (c) highly resolved C1 s spectra.

(COO^-), respectively. The bands at 1269 and 1020 cm^{-1} are due to the stretching vibrations of C-O and C-O-C, respectively. The bands at 932 and 554 cm^{-1} respectively are owing to the out-of-plane ring bend of C-OH and the wagging vibration of the COO^-. The band at 450 cm^{-1} is related to the Ni-O stretching vibration of NiO_6 octahedral in the cubic NiO structure, while the band at 668 cm^{-1} is

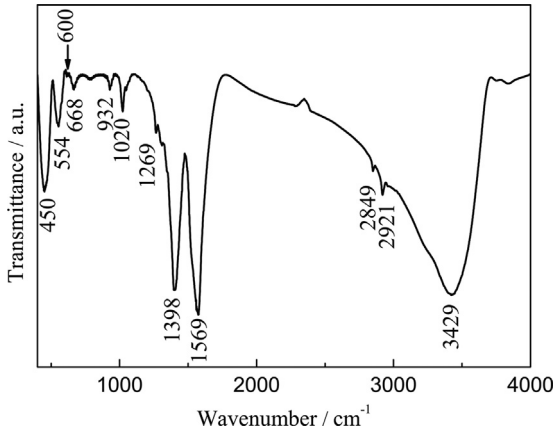

Figure 5 FTIR spectra of the NiO nanoparticles.

the characteristic of the stretching vibration of hydroxyl groups hydrogen bonded to Ni-O. In addition, higher valence (Ni^{3+}-O) stretching vibration mode can also be observed at 600 cm^{-1}, which matches well with the previous literatures [35-38].

Based on the above analysis, there are many functional groups such as alcohols, hydroxyl groups, and carboxyl at the contact interface between the seed layer and the NiO nanoparticles. During the solvothermal process, the carboxyl at the contact interface results in negative charge, Ni^{2+} ion is selectively bonded with it through mutual electrostatic attraction. In contrast to the negative charge of the NiO seed layer with carboxyl group, a reversal of the surface charge of NiO seed layer can be achieved by the adsorption of nickel ions at the surface. NiO surface is therefore alternatively positively charged or negatively charged. In either case the surface will attract ions of opposite charges to it, and this new surface covered with ions will in turn attract ions with opposite charges to cover the surface next and thereby reacting to form NiO. Therefore, the chemical bonding between the NiO and the substrate is very stable. In addition, the alkyl carboxylates can serve as capping ligands to from uniform NiO nanoparticles [24].

Electrochemical performance evaluations

Figure 6a shows typical CV curves of the NiO nanoparticles grown on nickel foam in a 1 M KOH electrolyte between 0 and 0.6 V at various scan rates ranging from 5 to 100 mV/s. The mass loading of the electrode is 0.5 mg cm^{-2}. A pair of redox current peaks with symmetrical shape was observed in each curve. Generally, CV curves appear nearly rectangular for electric double-layer capacitors; however, large redox current peaks are present for pseudocapacitor. The results indicate a typical pseudocapacitive behavior arising from the reversible Faradaic redox reactions between Ni^{2+} and Ni^{3+}. The electrochemical reaction is given as below [39,40]

$$NiO + OH^- \leftrightarrow NiOOH + e^- \quad (1)$$

As the scan rate increases from 5 to 100 mV/s, the current subsequently increases with a shift of oxidation peaks to a more positive position and reduction peaks to a more negative position due to the internal resistance of the

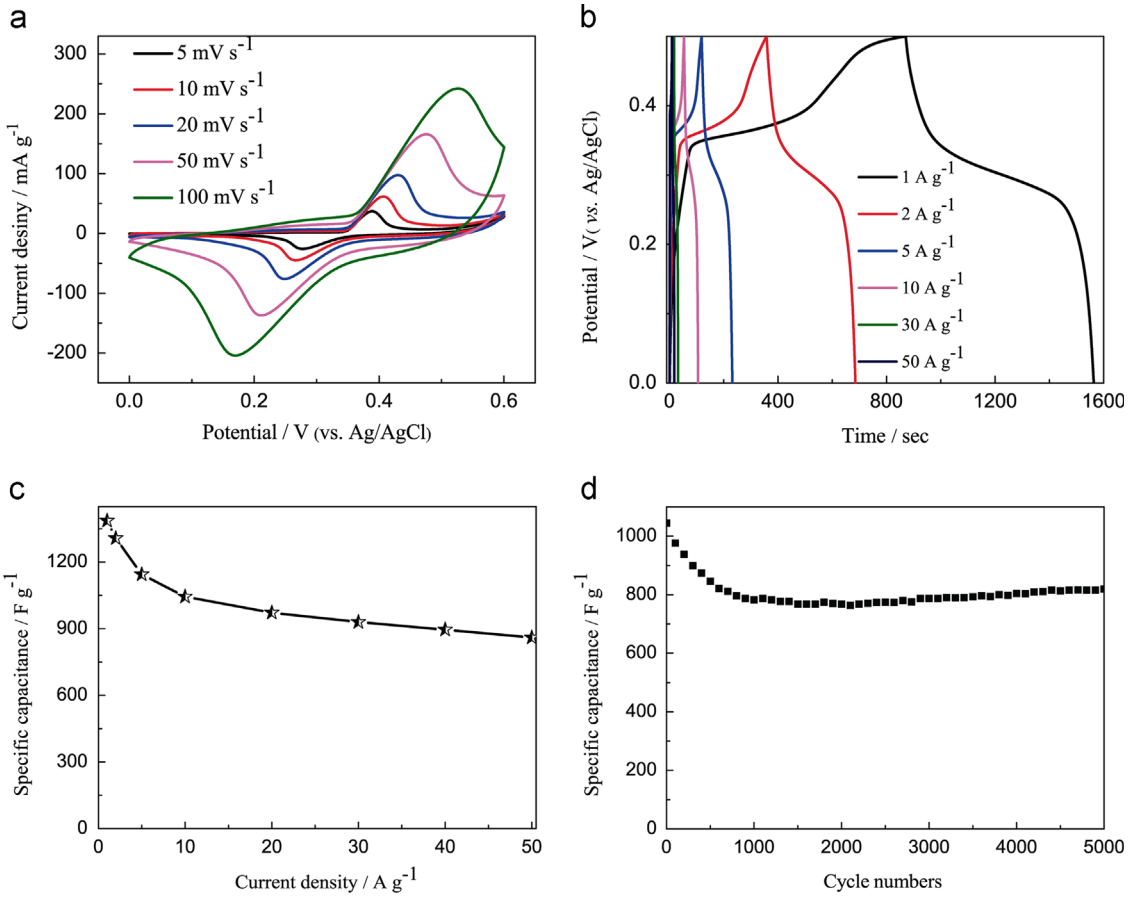

Figure 6 (a) Cyclic voltammograms of NiO nanoparticles film on nickel foam as working electrode in 1 M KOH at various scan rates in the potential range of 0–0.6 vs. Ag/AgCl. (b) Galvanostatic charge/discharge profiles for NiO nanoparticles film on nickel foam under different currents density in the potential range of 0–0.5 V (ranging from 1 to 50 A g^{-1}). (c) Specific capacitance of the NiO nanoparticles film as a function of the current density. (d) Cycle performance of the NiO nanoparticles film measured at 10 A g^{-1} for 5000 cycles.

electrode, but the very well-defined sharp redox reaction peaks are still maintained even at the high scanning rate of 100 mV s^{-1}, verifying a good electrochemical capacitive nature, low internal resistance and fast charge transfer in the film. In addition, the symmetric redox peaks indicates that the reaction reversibility for the NiO nanoparticles film is excellent.

To further evaluate the electrochemical properties and the application of the NiO nanoparticles film on supercapacitor, galvanostatic charging and discharging were performed using a Pt foil as counter electrode and Ag/AgCl as the reference electrode in 1 M KOH solution. Figure 6b shows the charge/discharge behaviors of the NiO nanoparticles film at different current densities, with the upward lines corresponding to charging and downward ones for discharging. The specific capacitance is calculated according to the following equation [41]:

$$C = \frac{I\Delta t}{M\Delta V} \tag{2}$$

where C (F g^{-1}) is the specific capacitance, I (mA) represents the discharge current, and M (mg), ΔV (V) and Δt (s) designate the mass of active materials, potential drop during discharge and total discharge time, respectively. The NiO (theoretical value is 2573 F g^{-1} within 0.5 V) nanoparticles film exhibits specific capacitance of 1386, 1307, 1145, 1044, 930 and 860 F g^{-1} at 1, 2, 5, 10, 30 and 50 A g^{-1}, respectively, which is much higher than the values of previously reported NiO pseudocapacitive nanomaterials [42–45]. Figure 6c shows the dependence of specific capacitance on current density for the NiO nanoparticles film. It is obvious that the specific capacitance decreases gradually with increasing discharge current density, which can be attributed to ions diffusing and migrating into the active materials adequately at low current density. At high current density, some active surface areas of the active materials become inaccessible for charge storage due to the diffusion effect, limiting the migration of the electrolytic ions. The specific capacitance of the NiO nanoparticles film decreases to 860 F g^{-1} as the current density increases to 50 A g^{-1}, only a 38% decrease compared with the specific capacitance at the current density of 1 A g^{-1}, indicative of excellent rate capability or capacitive behaviors under high current charge/discharge conditions. Long term cycling stability is another critical parameter for electrode materials. The NiO nanoparticles film showed satisfactory cycling stability in addition to ultrahigh specific capacitance and rate capacitance. The capacitance retains 78.5% at a high current

density of 10 A g^{-1} for 5000 cycles as shown in Figure 6d. Previous work on NiO nanorods synthesized by the hydrothermal method showed a maximum specific capacitance as high as 2018 F g^{-1} at 2.27 A g^{-1}. However, the NiO nanorods required a subsequent thermal treatment after hydrothermal and only 500 cycling stability has been presented [46]. The high capacitance, excellent rate capability and good cycling stability in our present work may be attributed to the uniform nanoparticles morphology and stable chemical bonding of the NiO nanoparticle on the Ni substrate. In the case of nanoparticles, the smallest dimension is represented by the ion diffusion length. Therefore, nanoparticles can provide a larger electrode–electrolyte contact area and shortens the ion diffusion length. The cycling stability can be a concern for the practical application of electrochromic materials.

The above results demonstrate that the NiO nanoparticles grow on nickel foam exhibits excellent supercapacitive properties. In addition, we envisioned that the NiO nanoparticles grown on ITO glass with NiO seed layer assisted could have outstanding properties in electrochromism. The film electrodes were colored by applying step voltages of 0.6 V and bleached by applying step voltage of −0.2 V (vs. Ag/AgCl). The color of the NiO film changed from brown (colored state) to transparent (bleached state). Figure 7a shows the transmittance spectra of the NiO nanoparticles film with seed layer between the colored and bleached states measured in the wavelength range of 300–900 nm. The NiO nanoparticles film with seed layer presents noticeable electrochromism with variation of transmittance up to 63.6% at 550 nm which is larger than that of the NiO film without seed layer (21% at 550 nm as shown in Figure S2 in Supporting information). The digital photos of NiO film growning on ITO glass with seed layer in bleached state and colored state are shown in the inset of Figure 7a. An important parameter of electrochromism is the switching time from one state to another state under alternating potentials. The switching time is defined as the time required for a system to reach 90% of its full optical modulation. Figure 7b and c reveals CA measurements and corresponding in situ transmittance at 550 nm, respectively. For the NiO nanoparticles film, the switching time for coloration and bleaching is 11.5 and 9.5 s respectively, which is comparable to the porous NiO nanosheet array film (9.1 and 13.3 s) [47]. *CE* is another important parameter for comparing different electrochromic materials, which is defined as the change in optical density (ΔOD) per unit of charge (ΔQ) intercalated into the electrochromic materials. It can be calculated from the following formulas [48]:

$$CE(\lambda) = \frac{\Delta OD(\lambda)}{\Delta Q} \tag{3}$$

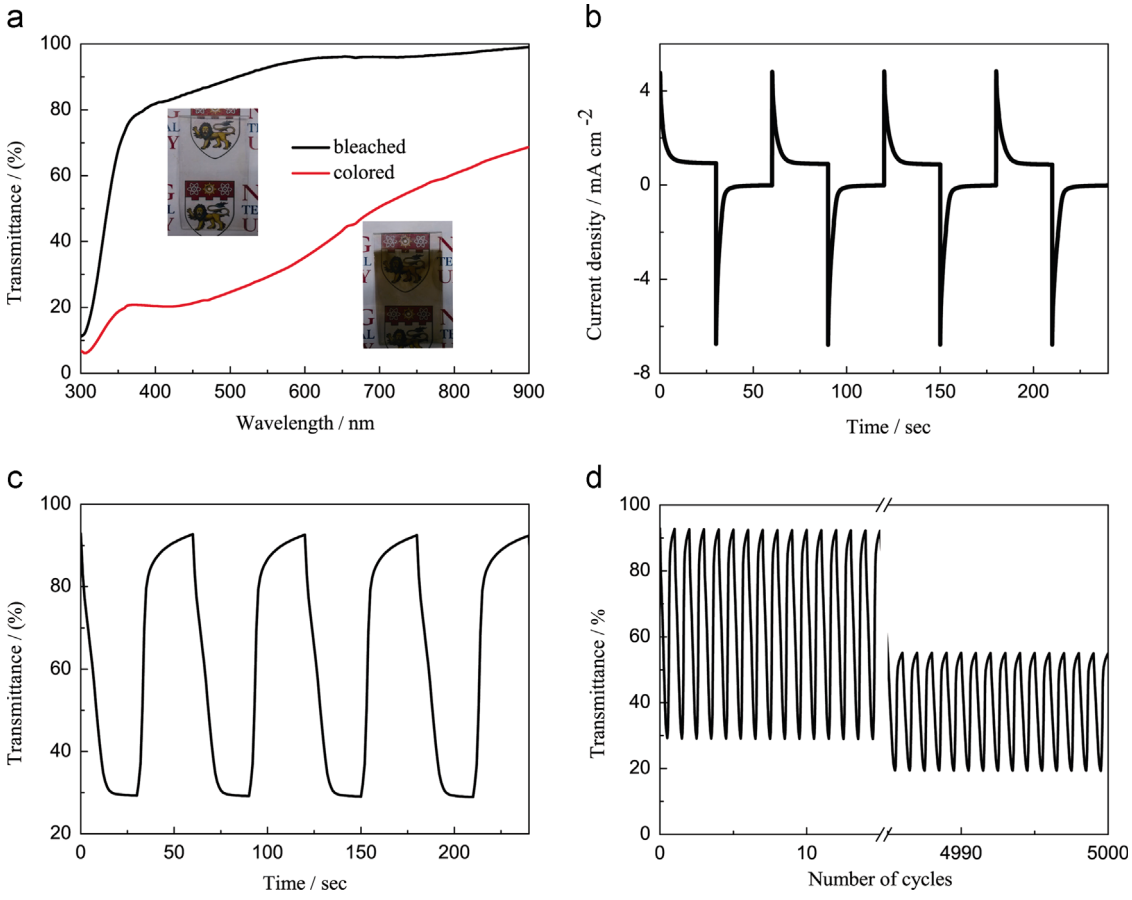

Figure 7 (a) Transmittance spectra of the NiO nanoparticles film with seed layer on ITO glass in the bleached (−0.2 V) and colored (0.6 V) states in the wavelength range of 300–900 nm (the digital photos of NiO film growing on ITO glass with seed layer on bleached state and colored state are presented in inset). (b) Current response for NiO nanoparticles film at −0.2 and 0.6 V applications in 1 M KOH for 30 s per step. (c) Corresponding in situ optical responses of NiO films for 30 s per step measured at 550 nm. (d) Cycle performance of the NiO nanoparticles film measured in 1 M KOH for 5000 cycles.

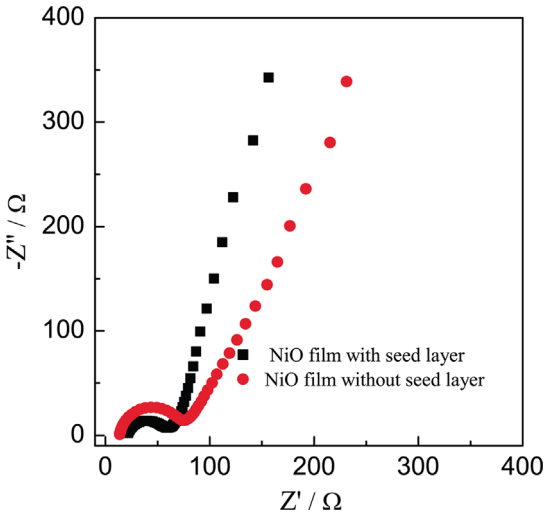

Figure 8 Nyquist plots of the NiO nanoparticles films with and without seed layer.

$$\Delta OD(\lambda) = \log \frac{T_b}{T_c} \quad (4)$$

where T_b and T_c denote transmittance in bleached and colored states, respectively. Usually, a high value of coloration efficiency indicates that the electrochromic materials exhibit large optical modulation with a small intercalation charge density. In this work, the value of coloration efficiency of the NiO nanoparticles film with seed layer is calculated about 42.8 $cm^2\ C^{-1}$ at 550 nm. The durability of NiO nanoparticle film was evaluated by chronoamperometry measurements and corresponding in-situ transmittance at 550 nm. Figure 7d shows the colored and bleached transmittance graph at 550 nm, which vary as a function of cycle number. The NiO nanoparticles film sustain a transmittance modulation of about 90.8% of their initial value after subjected for 1000 cycles, and sustains a transmittance modulation of about 56.4% even when subjected to 5000 cycles. The NiO nanoparticles film is more stable during cycling than the NiO nanosheet film [49] and nanorods film [50] previously reported. Therefore, the transmittance results verify that the NiO nanoparticles film has the outstanding stable, reversible and persistent electrochromic effects.

To further understand the electrochemical behavior and the chemical compatibility of the NiO nanoparticles film with seed layer, EIS measurements were conducted in a frequency range of 0.01 Hz to 100 kHz. EIS is a nondestructive and sensitive technique, widely used for the characterization of functionalized electrodes. Figure 8 shows the Nyquist diagrams obtained for the NiO nanoparticles films with and without seed layer. The Nyquist plots of both films consist of a slightly depressed semicircle in the high-frequency and a straight line in the low-frequency region. The semicircle corresponding to the charge-transfer resistance of electrochemical reaction and the line can be ascribed to the diffusion-controlled Warburg impedance. According to previous reports [51], the larger semicircle means a higher charge-transfer resistance, and a steeper slope indicates a faster ion-diffusion rate. Apparently, the NiO nanoparticles film with seed layer exhibits a smaller

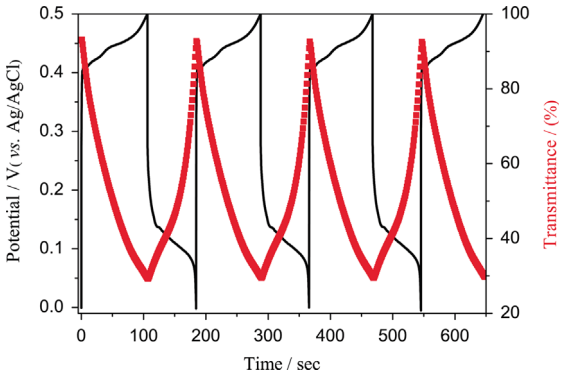

Figure 9 Galvanostatic charge/discharge profiles at 2 A g^{-1} in the potential range of 0–0.5 V and corresponding in situ optical responses measured at 550 nm for NiO nanoparticles film on ITO substrate with seed layer.

semicircle in high-frequency and more vertical straight line in the low-frequency, which indicates the lower charge-transfer resistance and faster ion diffusion behavior of the NiO nanoparticles film with seed layer than that of the NiO film without seed layer. Thus we can conclude that the seed layer can bridge the chemical compatibility between NiO nanoparticles and the ITO substrate.

As NiO film simultaneously functions in the energy storage and energy conservation electrochromic applications and shares the same electrochemical process in same electrolyte, it is very interesting to develop an energy storage device which is capable to sense changes in the level stored energy and can respond to these changes by visual changes [52,53]. To meet these needs, we test the charge/discharge curves and corresponding in situ transmittance at a current density of 550 nm at 2 A g^{-1} for NiO film grown on ITO glass with seed layer (Figure 9). The mass loading of the NiO film grown on ITO glass with seed layer is 0.15 mg cm^{-2}. The color of the films changes from transparent (bleached state) to brown (colored state) during charging process, then the color fades away during discharging process. When the NiO film is charged to 0.5 V, reaching a fully charged state, the color of the film is dark brown. In reverse process, when the electrical charge is completely consumed at a potential of 0 V, the film changed to transparent. Therefore, the energy storage stage can be visually monitored by the color change. Compared to the NiO film grown on nickel foam, the NiO film grown on ITO glass with seed layer exhibits lower specific capacitance (308 F g^{-1} at 2 A g^{-1}) which is mainly due to the poor conductivity of ITO glass than that of the nickel foam. Evidently, the specific capacitance of the NiO film grown on ITO glass with seed layer is much higher than that without seed layer (110 F g^{-1} at 2 A g^{-1} as shown in Figure S3 in Supporting information).

Conclusions

Uniform NiO nanoparticles on different substrates were successfully synthesized by a simple and low-cost solvothermal method. Electrochemical investigations revealed the excellent reaction reversibility and fast ion transport in charging and discharging for NiO nanoparticles electrodes,

and consequently an extremely excellent electrochromic performance was achieved, which sustained a transmittance modulation of about 56.4% even when subjected to 5000 cycles. The excellent electrochemical performance may be attributed to the uniform nanoparticles morphology and stable chemical bonding of the NiO nanoparticle on the substrates, which would shorten the ion diffusion length and greatly facilitate the charge transfer both at the contact interfaces and within the electrode materials during the electrochemical process. Moreover, we have demonstrated a novel smart supercapacitor electrode in which the energy storage stage can be visually monitored by the color change.

Acknowledgments

This research is supported by A*Star-MND Green Building Joint Grant 1321760013. Part of the work is also supported by NTU-HUJ-BGU Nanomaterials for Energy and Water Management Programme under the Campus for Research Excellence and Technological Enterprise (CREATE) that is supported by the National Research Foundation-Prime Minister's Office, Republic of Singapore.

Appendix A. Supporting information

Supplementary data associated with this article can be found in the online version at http://dx.doi.org/10.1016/j.nanoen.2014.12.031.

References

[1] P. Simon, Y. Gogotsi, Nat. Mater. 7 (2008) 845–854.
[2] S. Cong, Y.Y. Tian, Q.W. Li, Z.G. Zhao, F.X. Geng, Adv. Mater. 26 (2014) 4260–4267.
[3] K. Wang, H.P. Wu, Y.N. Meng, Y.J. Zhang, Z.X. Wei, Energy Environ. Sci. 5 (2012) 8384–8389.
[4] N. Lior, Renew. Sustain. Energy Rev. 18 (2013) 401–415.
[5] X. Wang, C. Yan, A. Sumboja, P.S. Lee, Nano Energy 3 (2014) 119–126.
[6] K. Wang, H.P. Wu, Y.N. Meng, Z.X. Wei, Small 10 (2014) 14–31.
[7] X. Wang, C.Y. Yan, A. Sumboja, J. Yan, P.S. Lee, Adv. Energy Mater. 4 (2014) 1301240.
[8] X.H. Xia, D.L. Chao, Z.X. Fan, C. Guan, X.H. Cao, H. Zhang, H.J. Fan, Nano Lett. 14 (2014) 1651–1658.
[9] J.Q. Sun, W.Y. Li, B.J. Zhang, G. Li, L. Jiang, Z.G. Chen, R.J. Zou, J.Q. Hu, Nano Energy 4 (2014) 56–64.
[10] D.T. Dam, X. Wang, J.-M. Lee, Nano Energy 2 (2013) 1303–1313.
[11] C.G. Granqvist, Adv. Mater. 15 (2003) 1789–1803.
[12] C.G. Granqvist, Sol. Energy Mater. Sol. Cells 92 (2008) 203–208.
[13] C.G. Granqvist, Sol. Energy Mater. Sol. Cells 99 (2012) 1–13.
[14] J.A. Lee, M.K. Shin, S.H. Kim, H.U. Cho, G.M. Spinks, G.G. Wallace, M.D. Lima, X. Lepró, M.E. Kozlov, R. H. Baughman, S.J. Kim, Nat. Commun. 4 (2013) 1970.
[15] B. Wang, J.S. Chen, Z. Wang, S. Madhavi, X.W. Lou, Adv. Energy Mater. 2 (2012) 1188–1192.
[16] G.A. Niklasson, C.G. Granqvist, J. Mater. Chem. 17 (2007) 127–156.
[17] E. Ozkan Zayim, I. Turhan, F.Z. Tepehan, N. Ozer, Sol. Energy Mater. Sol. Cells 92 (2008) 164–169.
[18] M.M. Uplane, S.H. Mujawar, A.I. Inamdar, P.S. Shinde, A.C. Sonavane, P.S. Patil, Appl. Surf. Sci. 253 (2007) 9365–9371.
[19] B.A. Reguig, A. Khelil, L. Cattin, M. Morsli, J.C. Bernede, Appl. Surf. Sci. 253 (2007) 4330–4334.
[20] X.H. Xia, J.P. Tu, J. Zhang, X.L. Wang, W.K. Zhang, H. Huang, Sol. Energy Mater. Sol. Cells 92 (2008) 628–633.
[21] G.F. Cai, J.P. Tu, C.D. Gu, J.H. Zhang, J. Chen, D. Zhou, S.J. Shi, X.L. Wang, J. Mater. Chem. A 1 (2013) 4286–4292.
[22] S. Pilban Jahromi, N.M. Huang, M.R. Muhamad, H.N. Lim, Ceram. Int. 39 (2013) 3909–3914.
[23] Y. Li, M. Afzaal, P. O'Brien, J. Mater. Chem. 16 (2006) 2175–2180.
[24] X.Y. Liang, Q. Yi, S. Bai, X.L. Dai, X. Wang, Z.Z. Ye, F. Gao, F.L. Zhang, B.Q. Sun, Y.Z. Jin, Nano Lett. 14 (2014) 3117–3123.
[25] Y.X. Lu, L. Liu, W. Foo, S. Magdassi, D. Mandler, P.S. Lee, J. Mater. Chem. C 1 (2013) 3651–3654.
[26] Y.X. Lu, L. Liu, D. Mandler, P.S. Lee, J. Mater. Chem. C 1 (2013) 7380–7386.
[27] A.M. Soleimanpour, A.H. Jayatissa, G. Sumanasekera, Appl. Surf. Sci. 276 (2013) 291–297.
[28] D.-W. Kim, D.-W. Park, Surf. Coat. Technol. 205 (2010) S201–S205.
[29] K. Fominykh, J.M. Feckl, J. Sicklinger, M. Döblinger, S. Böcklein, J. Ziegler, L. Peter, J. Rathousky, E.-W. Scheidt, T. Bein, D. Fattakhova-Rohlfing, Adv. Funct. Mater. 24 (2014) 3123–3129.
[30] H.-S. Kim, J.-C. Woo, Y.-H. Joo, C.-I. Kim, Vacuum 93 (2013) 7–12.
[31] V.S. Vidhya, V. Malathy, T. Balasubramanian, V. Saaminathan, C. Sanjeeviraja, M. Jayachandran, Curr. Appl. Phys. 11 (2011) 286–294.
[32] J.C. Bernède, S. Houari, D. Nguyen, P.Y. Jouan, A. Khelil, A. Mokrani, L. Cattin, P. Predeep, Phys. Status Solidi A 209 (2012) 1291–1297.
[33] X. Sun, G.K. Wang, J.-Y. Hwang, J. Lian, J. Mater. Chem. 21 (2011) 16581–16588.
[34] S.Y. Han, D.H. Lee, Y.J. Chang, S.O. Ryu, T.J. Lee, C.H. Chang, J. Electrochem. Soc. 153 (2006) C382–C386.
[35] Z.G. Chen, H.L. Chen, H. Hu, M.X. Yu, F.Y. Li, Q. Zhang, Z.G. Zhou, T. Yi, C.H. Huang, J. Am. Chem. Soc. 130 (2008) 3023–3029.
[36] Y.C. Si, E.T. Samulski, Nano Lett. 8 (2008) 1679–1682.
[37] A.G. Al-Sehemi, A.S. Al-Shihri, A. Kalam, G.H. Du, T. Ahmad, J. Mol. Struct. 1058 (2014) 56–61.
[38] Z.F. Zhu, N. Wei, H. Liu, Z.L. He, Adv. Powder Technol. 22 (2011) 422–426.
[39] K.C. Liu, M.A. Anderson, J. Electrochem. Soc. 143 (1996) 124–130.
[40] C. Natarajan, H. Matsumoto, G. Nogami, J. Electrochem. Soc. 144 (1997) 121–126.
[41] X.F. Wang, D.B. Ruan, Z. You, Trans. Nonferr. Metals Soc. China 16 (2006) 1129–1134.
[42] Y.Q. Zhang, X.H. Xia, J.P. Tu, Y.J. Mai, S.J. Shi, X.L. Wang, C.D. Gu, J. Power Sources 199 (2012) 413–417.
[43] C.Z. Yuan, L.R. Hou, Y.L. Feng, S.L. Xiong, X.G. Zhang, Electrochim. Acta 88 (2013) 507–512.
[44] M.-S. Wu, C.-Y. Huang, K.-H. Lin, J. Power Sources 186 (2009) 557–564.
[45] X.H. Xia, J.P. Tu, Y.J. Mai, R. Chen, X.L. Wang, C.D. Gu, X.B. Zhao, Chem. – Eur. J. 17 (2011) 10898–10905.
[46] Z.Y. Lu, Z. Chang, J.F. Liu, X.M. Sun, Nano Res. 4 (2011) 658–665.
[47] G.F. Cai, J.P. Tu, J. Zhang, Y.J. Mai, Y. Lu, C.D. Gu, X.L. Wang, Nanoscale 4 (2012) 5724–5730.
[48] L.C. Chen, K.C. Ho, Electrochim. Acta 46 (2001) 2151–2158.
[49] G.F. Cai, J.P. Tu, D. Zhou, L. Li, J.H. Zhang, X.L. Wang, C.D. Gu, J. Phys. Chem. C 118 (2014) 6690–6696.

[50] R.A. Patil, R.S. Devan, J.-H. Lin, Y.-R. Ma, P.S. Patil, Y. Liou, Sol. Energy Mater. Sol. Cells 112 (2013) 91–96.
[51] B.G. Choi, M. Yang, W.H. Hong, J.W. Choi, Y.S. Huh, ACS Nano 6 (2012) 4020–4028.
[52] X.L. Chen, H.J. Lin, P.N. Chen, G.Z. Guan, J. Deng, H.S. Peng, Adv. Mater. 26 (2014) 4444–4449.
[53] Y.Y Tian, S. Cong, W.M. Su, H.Y. Chen, Q.W. Li, F.X. Geng, Z.G. Zhao, Nano Lett. 14 (2014) 2150–2156.

Guofa Cai received his B.S., M.S. and Ph.D degrees in School of Materials Science and Engineering respectively from Henan Polytechnic University, Wuhan University of Technology and Zhejiang University, PR China. Currently, he is a research fellow under the supervision of Assoc. Prof. Pooi See Lee in the School of Materials Science and Engineering, Nanyang Technological University (NTU), Singapore. Now, his research interests mainly focus on nanomaterials for electrochromic and energy storage applications.

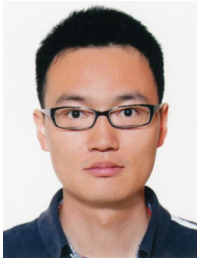

Xu Wang is currently a research staff in Assoc. Prof. Pooi See Lee's group. He completed his Ph.D. work under Prof. Lee focusing on the topic "metal oxide/hydroxide and their composite materials for supercapacitor application".

Mengqi Cui received her B.S. degree in 2012 from Jilin University, China. She is currently a Ph.D. candidate under the supervision of Prof. Pooi See Lee at the School of Materials Science and Engineering, Nanyang Technological University. Her research interests mainly focus on layer-by-layer deposition of polymeric complexes for electrochromic device applications.

Peter Darmawan received his Ph.D. from the School of Materials Science and Engineering (MSE) – Nanyang Technological University (NTU) in 2010. He specialized in the study of rare-earth oxides for gate dielectrics during his Ph.D. candidature. In August 2010, Peter relocated to National Institute for Materials Science (NIMS) International Center for Materials Architechtronics (MANA) in Japan for his post-doctoral research. At NIMS-MANA, he focused on reduction of contact resistance in organic electronics and metal oxide semiconductors and filed several patents. After 2 years in Japan, Peter rejoined NTU-MSE under the Nanomaterials for Energy and Water Management (NEW) CREATE Programme. His current research interests include transparent conductors, printed and flexible electronics and electrochromics.

Jiangxin Wang is Ph.D. student in the group of Prof. Pooi See Lee in the School of Materials Science and Engineering, Nanyang Technological University (NTU), Singapore. He obtained his B.S. degree in the School of Physical Electronics, University of Electronic Science and Technology of China (UESTC) in 2010. His current research interests focus on deformable optoelectronic devices.

Alice Lee-Sie Eh obtained her Master of Chemistry from Universiti Sains Malaysia in 2012. She is currently a Ph.D. candidate in Prof. Lee's group in the School of Materials Science and Engineering, Nanyang Technological University (NTU), Singapore. Her current research focus is in the field of electrochromics, polymer electrolytes and its applications. She has been working actively on both transmissive and reflective electrochromics devices in the past 2 years.

Pooi See Lee is an Associate Professor in the School of Materials Science and Engineering, Nanyang Technological University (NTU), Singapore. She obtained her B.Sc. (Hons) and Ph.D. at the National University of Singapore. Her research work focuses on the theme of electrochemical- and electrical-inspired devices based on nanostructures and nanocomposites, for applications in electrochromics, energy storages, actuators, ferroelectrics, electrical memory devices, sensors, flexible and stretchable electronics. She serves as the Associate Chair in the School of Materials Science and Engineering, NTU.